Acta Crystallographica Section D
Biological Crystallography
ISSN 0907-4449

The purification, crystallization and preliminary structural characterization of PhzF, a key enzyme in the phenazine-biosynthesis pathway from *Pseudomonas fluorescens* 2-79

Dmitri V. Mavrodi,[a] Nathalie Bleimling,[b] Linda S. Thomashow[a,c] and Wulf Blankenfeldt[b]*

[a]Department of Plant Pathology, Washington State University, Pullman, Washington 99164-6430, USA, [b]Max-Planck-Institute of Molecular Physiology, Otto-Hahn-Strasse 11, 44227 Dortmund, Germany, and [c]USDA Agricultural Research Service, Root Disease and Biological Control Research Unit, Pullman, Washington 99164-6430, USA

Correspondence e-mail: wulf.blankenfeldt@mpi-dortmund.mpg.de

Received 23 September 2003
Accepted 6 November 2003

Phenazines produced by members of several bacterial genera are biologically active metabolites that function in microbial competitiveness, the suppression of soil-borne plant diseases and virulence in infectious disease. Despite recent progress towards understanding the biochemistry of phenazine synthesis, the key reactions leading to the formation of the heterocyclic scaffold common to all phenazine compounds remain obscure. *Pseudomonas fluorescens* 2-79 contains seven phenazine (*phz*) genes that encode components of the pathway for biosynthesis of phenazine-1-carboxylic acid. A central step in this pathway involves the condensation of two identical precursor molecules derived from chorismic acid and is catalysed by the product of the *phzF* gene. In this study, recombinant PhzF was purified and crystallized from PEG 4000/ammonium sulfate/sodium citrate pH 5.6. The crystals belong to space group $P3_121$ or $P3_221$, with unit-cell parameters $a = b = 56.3$, $c = 156.4$ Å. They contain one monomer in the asymmetric unit and diffract to better than 1.7 Å on synchrotron beamlines. Crystals of seleno-L-methionine-labelled PhzF have been obtained and SAD data are reported.

1. Introduction

Naturally occurring phenazines encompass a group of water-soluble nitrogen-containing aromatic pigments produced by members of several bacterial genera including *Pseudomonas*, *Erwinia, Burkholderia*, *Brevibacterium* and *Streptomyces* (Giddens *et al.*, 2002; Smirnov & Kiprianova, 1990; Turner & Messenger, 1986). Almost all phenazines exhibit broad-spectrum activity against Gram-positive and Gram-negative bacteria as well as fungi and higher animal and plant tissues (Smirnov & Kiprianova, 1990). These antibiotic properties are thought to be a consequence of the ability of phenazine compounds to undergo oxidation–reduction transformations and to act as electron acceptors that interfere with the functioning of the respiratory chain (Hassan & Fridovich, 1980). Phenazine compounds produced by root-associated fluorescent *Pseudomonas* spp. function in the suppression of soil-borne plant pathogens (Pierson & Thomashow, 1992; Thomashow & Weller, 1988). Recent studies have demonstrated that phenazine production is required for the generation of pathogenic symptoms in plants and higher animals as well as for effective nematode killing by *P. aeruginosa* (Mahajan-Miklos *et al.*, 1999; Rahme *et al.*, 1997). These observations suggest that phenazines act as broad-spectrum antibiotics and pathogenicity factors that may contribute to the survival of phenazine-producing strains in natural habitats.

Studies of phenazine-biosynthetic operons from *P. aureofaciens/chlororaphis* (Chin-A-Woeng *et al.*, 2001; Pierson *et al.*, 1995), *P. fluorescens* (Mavrodi *et al.*, 1998) and *P. aeruginosa* (Mavrodi *et al.*, 2001) have demonstrated that the 'core' biosynthetic pathway consists of seven unique *phz* genes that confer the ability to synthesize phenazine-1-carboxylic acid. The products of *phz*C, *phzD* and *phzE* are similar to enzymes of shikimic and chorismic acid metabolism. Together with PhzF and PhzG, they are absolutely necessary for phenazine production (Fig. 1; McDonald *et al.*, 2001). Owing to the lack of sequence similarity of the Phz enzymes PhzA, PhzB and PhzF to proteins of known function, however, the interesting chemistry leading to the phenazine scaffold is still not fully understood. With the exception of the isochorismatase PhzD from *P. aeruginosa*, which has recently been described in the literature (Parsons *et al.*, 2003), structural knowledge of the Phz enzymes has not been accumulated. We therefore have embarked on a program aimed at providing detailed structural insight into phenazine biosynthesis.

The key step in this pathway involves condensation of two identical precursor molecules, most probably 2,3-dihydro-3-oxo-anthranilic acid (McDonald *et al.*, 2001). The reaction can be carried out, albeit inefficiently,

by the enzyme PhzF alone. PhzF from *P. fluorescens* is a 278-residue protein that lacks a detectable sequence relationship with any protein in the PDB (Berman *et al.*, 2000). By using the fold-recognition program *3D-PSSM* (Kelley *et al.*, 2000) and more exhaustive BLAST searches (Altschul *et al.*, 1997) as well as searches against HMM-based domain databases (Pfam, TIGRFAMs), however, it becomes clear that PhzF exhibits significant similarity to diaminopimelate epimerases, which belong to a fold family that, with only two representatives (Cirilli *et al.*, 1998; Roper *et al.*, unpublished work), is strongly underrepresented in the structural database. Interestingly, PhzF lacks the conserved cysteines that are located at the active site of members of this PLP-independent amino-acid racemase family, which separates the enzyme from diaminopimelate epimerases, and raises unresolved questions about the exact mechanism of the phenazine-ring condensation.

We report here the large-scale expression of recombinant *P. fluorescens* PhzF and the first diffraction data collected from high-quality protein crystals as an initial step towards understanding the reaction mediated by PhzF.

2. PhzF overexpression and purification

A 866 bp DNA fragment containing *phzF* from *P. fluorescens* 2-79 was generated by PCR with the oligonucleotide primers phzF-up (5′-TTT CAT ATG CAC AAC TAC GTC AT-3′) and phzF-low (5′-TTT GGA TCC TTG TAT TGA GCC GTT-3′). The PCR product was digested with *Nde*I and *Bam*HI, gel-purified, cloned behind a T7 promoter in the N-terminal His-tag fusion vector pET-15b (Novagen) and single-pass sequenced to confirm the integrity of the resultant fusion. In pET-15b, the N-terminal His tag can be removed with thrombin. However, the cleavage site proved to be inaccessible and the PhzF fusion protein was purified from cultures of *Escherichia coli* Rosetta (DE3)/pLysS (Novagen) in the uncleaved form. Briefly, *E. coli* harbouring the recombinant plasmid was grown at 310 K in Terrific Broth media containing 100 µg ml^{-1} ampicillin and 34 µg ml^{-1} chloramphenicol to an OD_{600} of 0.6 and then induced with 1 m*M* isopropyl-β-D-thiogalactopyranoside (IPTG) for 3 h. The cells were harvested by centrifugation (30 min, 7000*g*, 277 K) and suspended in a buffer containing 50 m*M* sodium phosphate pH 8.0, 150 m*M* NaCl, 5 m*M* β-mercaptoethanol and 10%(*v*/*v*) glycerol. PMSF (5 m*M*) and DNAse I (20 µg ml^{-1}) were added and the cells were disrupted in a microfluidizer. The lysate was cleared by ultracentrifugation (150 000*g*, 45 min, 277 K) and then passed through a HiTrap Chelating HP column (Amersham Biosciences) that had been charged with 100 m*M* $NiSO_4$ and equilibrated with the lysis buffer. The column was washed with the same buffer supplemented with 20 m*M* imidazole on an ÄKTA Prime chromatography system (Amersham Biosciences) and bound proteins were eluted by washing sequentially with buffers containing 50, 100, 200 and 500 m*M* concentrations of imidazole. Fractions containing pure recombinant PhzF were identified by SDS–PAGE, pooled and concentrated by ultrafiltration to 20 mg ml^{-1} as determined by Bradford assay (Bradford, 1976). Buffer exchange and removal of aggregated proteins was achieved on a Superdex 75 gel-filtration column (Amersham Biosciences) run with 20 m*M* Tris–HCl pH 8.0, 150 m*M* NaCl, 2 m*M* β-mercaptoethanol, 10%(*v*/*v*) glycerol. Recombinant PhzF eluted as a monomer. MALDI–TOF mass-spectrometry analysis of the purified protein shows the presence of nearly equal amounts of two species with $(M + H)^+$ masses of 32 048 and 32 224, respectively. This indicates that part of the protein has been N-terminally processed (the expected mass after cleavage of the N-terminal methionine is 32 066), whereas the heavier species can be attributed to partial oxidation, probably of the N-terminal methionine (the expected mass for the full-length protein is 32 197). The purified protein was concentrated to 20 mg ml^{-1} and stored in small aliquots at 192 K.

As molecular-replacement studies using coordinates of the related protein diaminopimelate epimerase were unsuccessful, experimental phasing using SAD or MAD was initiated. Seleno-L-methionine was incorporated into PhzF during inhibition of methionine biosynthesis in synthetic media (Doublié, 1997). *E. coli* Rosetta (DE3)/pLysS cells bearing pET-15b with 6×His-tagged PhzF were grown overnight in Luria–Bertani media supplemented with ampicillin and chloramphenicol, pelleted and suspended in M9 media amended with 50 µg ml^{-1} ampicillin and 17 µg ml^{-1} chloramphenicol. The culture was grown at 310 K to mid-log phase (OD_{600} of 0.8) and amino acids (lysine, phenylalanine and threonine to 100 mg l^{-1}; isoleucine, leucine and valine to 50 mg l^{-1}) were added. The culture was supplemented with 60 mg l^{-1} seleno-L-methionine and allowed to cool to 292 K before overnight induction with 1 m*M* IPTG. The labelled protein showed purification properties identical to the native enzyme. Incorporation of selenium was confirmed by MALDI mass spectrometry.

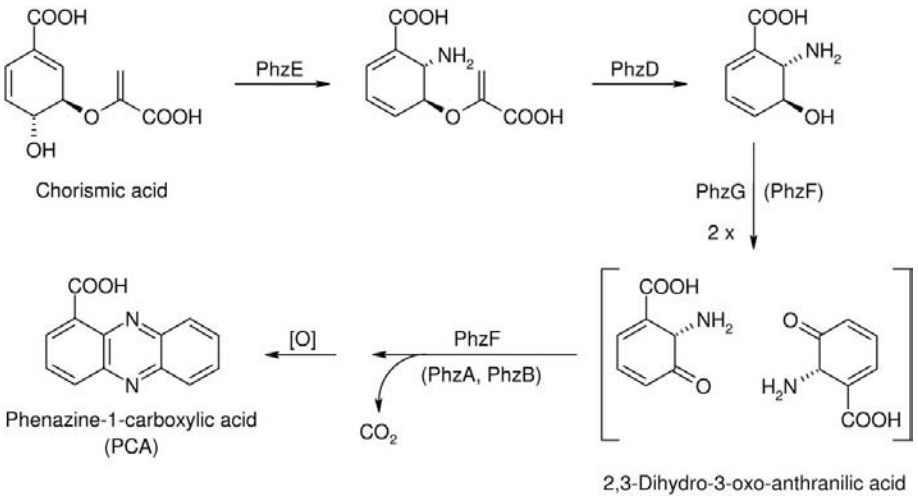

Figure 1
Biosynthesis pathway for phenazine-1-carboxylic acid in *P. fluorescens* as proposed by McDonald *et al.* (2001).

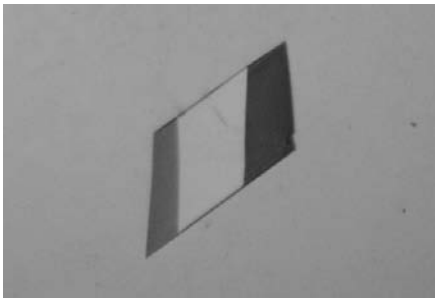

Figure 2
Photograph of a native PhzF crystal (approximate dimensions 0.3 × 0.3 × 0.2 mm).

Table 1
Data-collection statistics.

Values in parentheses are for the highest resolution shell.

	Native	SeMet-SAD
Wavelength (Å)	1.542 (rotating anode)	0.934 (ID14-EH1)
Resolution (Å)	20–1.94 (2.06–1.94)	30–1.70 (1.80–1.70)
Space group	$P3_{2/1}21$	$P3_{2/1}21$
Unit-cell parameters (Å)	$a = b = 56.6$, $c = 157.3$	$a = b = 56.3$, $c = 156.4$
V_M (Å^3 Da^{-1})	2.26	2.22
Total measurements	91552	658746
Unique reflections	21399	31965
Average redundancy	4.3 (4.3)	20.6 (15.3)
$I/\sigma(I)$	18.7 (6.7)	27.4 (9.8)
Completeness (%)	95.2 (89.3)	98.2 (91.1)
Anomalous completeness† (%)	—	98.3 (90.9)
Wilson B (Å^2)	28	22
R_{sym}‡ (%)	4.6 (19.6)	7.5 (26.8)

† Completeness calculations treat Friedel pairs as separate observations. ‡ $R_{sym} = \sum |I(h)_j - \langle I(h)\rangle| / \sum I(h)_j$, where $I(h)_j$ is the scaled observed intensity of the ith symmetry-related observation of reflection h and $\langle I(h)_i\rangle$ is the mean value.

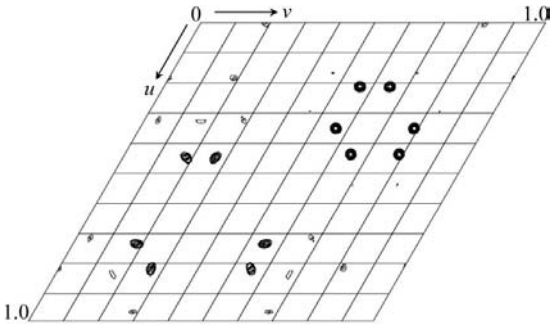

Figure 3
Harker section $w = 1/3$ of the Patterson map calculated with the anomalous differences of the SAD data (all data included, map contoured at 3σ). The figure was prepared with programs from the *CCP*4 package (Collaborative Computational Project, Number 4, 1994).

3. PhzF crystallization

Initial crystallization conditions were determined with Crystal Screen and Crystal Screen 2 from Hampton Research (Jancarik & Kim, 1991; Cudney *et al.*, 1994). The protein concentration was screened at 20, 10 and 5 mg ml^{-1} by dilution of the protein stock with Milli-Q water. The hanging-drop vapour-diffusion method with drops consisting of 1 µl protein and 1 µl precipitant solution at room temperature was used throughout. Conditions that produced microcrystalline precipitates were optimized with respect to precipitant concentration and pH in order to reduce the amount of nucleation and increase the size and appearance of crystals obtained. As these experiments showed a clear preference for polyethylene glycols in the presence of salts buffered in the pH range 5.0–5.6, a PEG/Ion Screen (Hampton Research) buffered with 0.1 *M* sodium citrate pH 5.4 was carried out. This illustrated the need to include medium-sized anions in the crystallization reagent, as crystals were only obtained with phosphate, sulfate, acetate and tartrate salts, whereas the nature of cations was found not to be important. Diffraction-quality crystals were obtained using a protein concentration of 5 mg ml^{-1} and a reservoir consisting of 100 m*M* sodium citrate pH 5.6, 200 m*M* $(NH_4)_2SO_4$ and 8–12%(*w*/*v*) PEG 4000. The colourless crystals possess an oblique shape and grow to dimensions of 0.3 × 0.3 × 0.2 mm (Fig. 2).

4. Data collection

To achieve cryoprotection, crystals were washed briefly in mother liquor supplemented with either 10%(*w*/*v*) sucrose and 10%(*w*/*v*) xylitol (native data set) or 30%(*v*/*v*) glycerol (SAD data set) prior to flash-cooling in liquid nitrogen. A data set was collected from a native protein crystal at 100 K as 145 non-overlapping 10 min 0.5° oscillation images on an Enraf–Nonius FR591 rotating-anode generator equipped with Osmic mirrors and a MAR 345 imaging plate. SAD data from a selenomethionine-labelled crystal were collected at 100 K from 720 non-overlapping 0.5° oscillations on beamline ID14-EH1 of the ESRF (Grenoble, France) using a Quantum-ADSC detector with 1 s exposure time in three passes per image. As this beamline cannot be tuned for optimal anomalous data collection, care was taken to obtain highly redundant and non-overlapped data, which, owing to the relatively long *c* axis of 156.4 Å, meant cutting back on resolution. All data were indexed, integrated and scaled with the *XDS* package (Kabsch, 1993). The crystals diffract to better than 1.7 Å resolution (Table 1) and systematic absences reveal that they belong to space group $P3_121$ or $P3_221$ with one monomer per asymmetric unit, corresponding to a V_M of 2.26 Å^3 Da^{-1} (Matthews, 1968). The SAD data contain a significant anomalous signal, giving rise to strong peaks (>5σ) in the Harker sections of the anomalous difference Patterson map (Fig. 3). However, these peaks are indicative of only two out of nine possible anomalous scatterers, which may be because of the non-optimal wavelength of the beamline used for data collection. We are nevertheless currently using these data to determine the position of Se atoms and derive initial phases for electron-density calculation.

We are thankful to I. Schlichting and R. S. Goody for encouraging discussions. The use of beamlines at the ESRF, Grenoble (France) is gratefully acknowledged.

References

Altschul, S. F., Madden, T. L., Schäffer, A. A., Zhang, J., Zhang, Z., Miller, W. & Lipman, D. J. (1997). *Nucleic Acids Res.* **25**, 3389–3402.
Berman, H. M., Westbrook, J., Feng, Z., Gilliland, G., Bhat, T. N., Weissig, H., Shindyalov, I. N. & Bourne, P. E. (2000). *Nucleic Acids Res.* **28**, 235–242.
Bradford, M. M. (1976). *Anal. Biochem.* **72**, 248–252.
Chin-A-Woeng, T. F. C., Thomas-Oates, J. E., Lugtenberg, B. J. J. & Bloemberg, G. V. (2001). *Mol. Plant-Microbe Interact.* **14**, 1006–1015.
Cirilli, M., Zheng, R., Scapin, G. & Blanchard, J. S. (1998). *Biochemistry*, **37**, 16452–16458.
Collaborative Computational Project, Number 4 (1994). *Acta Cryst.* D**50**, 760–763.
Cudney, R., Patel, S., Weisgraber, K., Newhouse, Y. & McPherson, A. (1994). *Acta Cryst.* D**50**, 414–423.
Doublié, S. (1997). *Methods Enzymol.* **276**, 523–530.
Giddens, S. R., Feng, Y. & Mahanty, H. K. (2002). *Mol. Microbiol.* **45**, 769–783.
Hassan, H. M. & Fridovich, I. (1980). *J. Bacteriol.* **141**, 156–163.
Jancarik, J. & Kim, S.-H. (1991). *J. Appl. Cryst.* **24**, 409–411.
Kabsch, W. (1993). *J. Appl. Cryst.* **26**, 795–800.
Kelley, L. A., MacCallum, R. M. & Sternberg, M. J. E. (2000). *J. Mol. Biol.* **299**, 499–520.
McDonald, M., Mavrodi, D. V., Thomashow, L. S. & Floss, H. G. (2001). *J. Am. Chem. Soc.* **123**, 9459–9460.
Mahajan-Miklos, S., Tan, M.-W., Rahme, L. G. & Ausubel, F. M. (1999). *Cell*, **96**, 47–56.
Matthews, B. W. (1968). *J. Mol. Biol.* **33**, 491–497.
Mavrodi, D. V., Bonsall, R. F., Delaney, S. M., Soule, M. J., Phillips, G. & Thomashow, L. S. (2001). *J. Bacteriol.* **183**, 6454–6465.
Mavrodi, D. V., Ksenzenko, V. N., Bonsall, R. F., Cook, R. J., Boronin, A. M. & Thomashow, L. S. (1998). *J. Bacteriol.* **180**, 2541–2548.
Parsons, J. F., Calabrese, K., Eisenstein, E. & Ladner, J. E. (2003). *Biochemistry*, **42**, 5684–5693.
Pierson, L. S. III, Gaffney, T., Lam, S. & Gong, F. (1995). *FEMS Microbiol. Lett.* **134**, 299–307.
Pierson, L. S. III & Thomashow, L. S. (1992). *Mol. Plant-Microbe Interact.* **5**, 330–339.
Rahme, L. G., Tan, M.-W., Le, L., Wong, S. M., Tompkins, R. G., Calderwood, S. B. & Ausubel, F. M. (1997). *Proc. Natl Acad. Sci. USA*, **94**, 13254–13250.
Smirnov, V. V. & Kiprianova, E. A. (1990). *Bacteria of Pseudomonas Genus*, pp. 100–111. Kiev, Ukraine: Naukova Dumka.
Thomashow, L. S. & Weller, D. M. (1988). *J. Bacteriol.* **170**, 3499–3508.
Turner, J. M. & Messenger, A. J. (1986). *Adv. Microb. Physiol.* **27**, 211–275.